Published in final edited form as:
Cell. 2013 August 1; 154(3): 676–690. doi:10.1016/j.cell.2013.07.006.

PQM-1 complements DAF-16 as a key transcriptional regulator of DAF-2-mediated development and longevity

Ronald G. Tepper[1], **Jasmine Ashraf**[2], **Rachel Kaletsky**[2], **Gunnar Kleemann**[2], **Coleen T. Murphy**[2,+], and **Harmen J. Bussemaker**[1,3,+]

[1]Department of Biological Sciences, Columbia University, New York, NY 10027, USA

[2]Lewis-Sigler Institute for Integrative Genomics and Dept. of Molecular Biology, Princeton University, Princeton, NJ 08544, USA

[3]Center for Computational Biology and Bioinformatics, Columbia University Medical Center, New York, NY 10027, USA

SUMMARY

Reduced insulin/IGF-1-like signaling (IIS) extends *C. elegans* lifespan by upregulating stress response (Class I) and downregulating other (Class II) genes through a mechanism that depends on the conserved transcription factor DAF-16/FOXO. By integrating genomewide mRNA expression responsiveness to DAF-16 with genomewide *in vivo* binding data for a compendium of transcription factors, we discovered that PQM-1 is the elusive transcriptional activator that directly controls development (Class II) genes by binding to the DAF-16 associated element (DAE). DAF-16 directly regulates Class I genes only, through the DAF-16 binding element (DBE). Loss of PQM-1 suppresses *daf-2* longevity and further slows development. Surprisingly, the nuclear localization of PQM-1 and DAF-16 is controlled by IIS in opposite ways, and was also found to be mutually antagonistic. We observe progressive loss of nuclear PQM-1 with age, explaining declining expression of PQM-1 targets. Together, our data suggest an elegant mechanism for balancing stress response and development.

INTRODUCTION

Reduced insulin/IGF-1-like signaling (IIS) greatly extends the lifespan of many organisms, including the nematode *C. elegans*. This effect is almost entirely dependent on activation of the FOXO transcription factor DAF-16 (Kenyon et al., 1993; Lin et al., 1997; Ogg et al., 1997). The IIS pathway is conserved, with increased longevity requiring the DAF-16 ortholog dFOXO in *Drosophila* and FOXO3A in mammals (Kenyon, 2005). Under normal conditions of nutrient availability and growth, AKT-dependent phosphorylation of specific amino acid residues causes DAF-16 to be retained in the cytosol and thus be

[+]Co-corresponding authors: hjb2004@columbia.edu, ctmurphy@princeton.edu.

ACCESSION NUMBERS The microarray data reported here are available at http://puma.princeton.edu under Experiment IDs 115871-73, 114875-79, and 116162-65.

AUTHOR CONTRIBUTIONS RT & HB performed all computational analyses, CTM designed all *C. elegans* experiments, RK & JA performed DAE promoter binding experiments, GK & JA performed dauer recovery experiment, JA performed all remaining experiments, and RT, HB, & CTM wrote the manuscript.

transcriptionally inactive (Berdichevsky et al., 2006; Lin et al., 1997; Ogg et al., 1997). Upon reduced insulin pathway signaling, AKT-dependent phosphorylation of DAF-16 decreases, promoting DAF-16 nuclear translocation, which leads to both upregulation and downregulation of large sets of genes, referred to as Class I and II, respectively (Murphy et al., 2003).

Identifying DAF-16 target genes and the processes they control is key to understanding the molecular and biochemical determinants of longevity and aging. Several studies have been performed to identify the genes regulated by DAF-16 (Halaschek-Wiener et al., 2005; Lee et al., 2003; McElwee et al., 2003; Murphy et al., 2003; Oh et al., 2006). Agreement on the identity of the targets, however, has been limited to a relatively small number of top responders (Murphy, 2006).

A core sequence required for *in vitro* binding by DAF-16 (GTAAACA or TGTTTAC), named the DAF-16 Binding Element (DBE), was determined using SELEX (Furuyama et al., 2000). This motif was found to be over-represented upstream of DAF-16 transcriptional targets (Murphy et al., 2003); the same study identified a second, GATA-like over-represented sequence (TGATAAG or CTTATCA), named the DAF-16 Associated Element (DAE).

A recent genome-scale *in vivo* binding assay suggested that DAF-16 exclusively acts as a transcriptional activator of Class I genes (Schuster et al., 2010), implying that a different *trans*-acting factor must be responsible for the DAF-16-dependent downregulation also observed in *daf-2* mutants. The identity of this complementary factor, however, has remained elusive (Budovskaya et al., 2008; Tonsaker et al., 2012; Zhang et al., 2013).

At the outset of this study, we reasoned that careful meta-analysis of all available genomewide differential expression profiles that contrast a condition in which DAF-16 is active (nuclear) with one in which it is inactive (cytosolic or null) would yield a valuable consensus definition of DAF-16 targets. To this end, we reprocessed relevant raw data from various laboratories. By integrating the evidence for differential expression from all these experiments using a voting algorithm developed specifically for this purpose, we were able to robustly score all *C. elegans* genes in terms of their responsiveness to the nuclear presence of DAF-16. This allowed us to define the significant positive (Class I) and negative (Class II) targets of DAF-16 with unprecedented sensitivity and specificity.

Our ranking by consensus DAF-16 responsiveness provided a framework for unraveling the *trans*-acting mechanisms underlying longevity. Integrating with a recent compendium of *in vivo* genomic binding sites for 46 transcription factors defined using ChIP-seq (Niu et al., 2011), we discovered that the transcription factor PQM-1 is highly significantly associated with DAE occurrence and with transcriptional response to DAF-16. A reporter gene assay confirmed PQM-1 as a *trans*-acting factor that activates transcription in a DAE-dependent manner.

Further detailed functional characterization demonstrated that *pqm-1* is required for *daf-2* longevity and stress response, and that the expression of DAF-16 targets is specifically affected by loss of *pqm-1*. The nuclear localization of PQM-1 is regulated by the IIS pathway and by stress conditions, but is anti-correlated with that of DAF-16. Surprisingly, nuclear localization of DAF-16 and PQM-1 is mutually antagonistic, which allows DAF-16 to indirectly influence the expression of Class II genes. *pqm-1* is required for normal development and dauer recovery, suggesting a role for PQM-1 in normal development as well. Finally, we observe a loss of nuclear localization of PQM-1 during normal aging, which seems to explain a broad but specific loss of gene expression with age.

Taken together, our data suggest that PQM-1 plays a central role in wide range of key biological phenomena, including normal development and aging, and the regulation of *daf-2*/IIS-mediated longevity.

RESULTS

A robust consensus definition of DAF-16-responsive genes

To determine which genes show mRNA-level response to changes in DAF-16 activity, we first collected all publicly available data from genomewide expression studies that explicitly contrast conditions with differing levels of DAF-16 activity (typically, *daf-2(−)* vs. *daf-16(−);daf-2(−)*). Next we developed a robust voting algorithm that allowed us to identify genes with consistent evidence of upor downregulation (Figure 1A). It classified 1663 genes as positive (Class I) and 1733 genes as negative (Class II) targets of DAF-16 at a 5% false discovery rate (Figure 1B; Supplemental Table S1). Of 22 genes with prior literature evidence of being DAF-16-responsive, we recovered 18 as significant ($P < 0.05$) and with the same direction of response (Supplemental Table S2). Furthermore, while the top-ranked Class I and Class II genes (Table 1) are enriched for previously identified targets, 52% of our predictions are novel. Together, these statistics illustrate the sensitivity and specificity of our method.

The most enriched Gene Ontology (GO) categories among Class I genes are “oxidation reduction”, consistent with previous findings that oxidative stress defenses are increased by DAF-16 (Honda and Honda, 1999; Murphy et al., 2003), and “carbohydrate metabolic process,” consistent with previous mass spectrometric analysis of *daf-2* mutants (Dong et al., 2007); Class II targets are highly enriched for genes involved in metabolism, growth, reproduction, and development (Supplemental Table S3). Using a set of genomewide gene-tissue predictions covering 13 major tissues (Chikina et al., 2009), we found Class I targets to be enriched for hypodermal genes and depleted for germ line-expressed genes, while Class I and II were both depleted for neuronal genes (Figure 1C). Class II targets are strongly and specifically enriched for intestinal genes (Figure 1C; Supplemental Figure S1A). Consistent with these observations, it has been shown that restoring DAF-16 solely in the intestine of *daf-2;daf-16*-deficient animals restores longevity by ~60% while neuronal DAF-16 activity extends lifespan by only ~10% (Libina et al., 2003), and that expression of *daf-16* in the hypodermis of *daf-16;daf-2* animals increases life span by 30% (Zhang et al., 2013).

An *in vivo* genomic binding profile for DAF-16 obtained using DamID (Schuster et al., 2010) confirms its specific association with Class I genes (Figure 1D and Supplemental Table S4); as previously noted by these authors, however, Class II genes show no enrichment for DAF-16 binding. Similarly, differential mRNA expression between wild-type and *daf-16(−)* is mostly confined to Class I genes (Figure 1E and Supplemental Table S4). (In contrast to this good agreement, a list of candidate DAF-16 targets from a ChIP-PCR-based analysis (Oh et al., 2006) is not enriched for either Class I or Class II targets (Supplemental Figure S1B), or for DBE or DAE sites (Murphy and Kenyon, 2006), perhaps due to the small number of clones (<200) analyzed in that study.)

Taken together, the above results strongly validate our consensus ranking of DAF-16 responsiveness at various biological levels. They also underscore the fact that DAF-16 specifically binds and regulates Class I targets, leaving as an open question what controls the expression of Class II genes.

Discovering cis-regulatory motifs that explain DAF-16 responsiveness

To reveal the *cis*-regulatory logic underlying the DAF-16 transcriptional network, we examined the responsiveness to changes in DAF-16 activity of each gene in terms of its upstream non-coding sequence. We exploited the fact that the degree of DAF-16 activation varies considerably over the set of experiments we analyzed. Using the difference in the mean mRNA expression log-ratio of the top 100 targets of DAF-16 in Class I and Class II, respectively, as a virtual reporter of its transcriptional activity (Boorsma et al., 2008), we quantified the responsiveness of each gene by performing least-squares regression across all experiments of its mRNA expression log-ratios on inferred DAF-16 activity.

To discover DNA motifs that explain the gene-to-gene variation in DAF-16 responsiveness, we used the *REDUCE* suite of software tools for cis-regulatory analysis (http://bussemakerlab.org/REDUCE/). We first ran the *MotifREDUCE* algorithm to perform an unbiased, exhaustive search of all oligonucleotides up to octamers for the motif that best predicted variation in DAF-16 responsiveness within the set of upregulated (Class I) and downregulated (Class II) targets. The canonical DBE (GTAAACA or TGTTTAC) emerged as the most predictive motif for the positive set, and the canonical DAE (TGATAAG or CTTATCA) as the best predictor for the negative set.

The regression framework of REDUCE provides the ability to determine how the effectiveness of DBE and DAE occurrences depends on their position relative to the transcription start site (TSS). Previous DAF-16 studies have assumed effective upstream promoter region sizes ranging from 1000 bp (Lee et al., 2003; McElwee et al., 2004; Murphy et al., 2003) to 3000 bp (McElwee et al., 2003) or even 5000 bp (Oh et al., 2006). We found that responsiveness to both the DBE and the DAE is largest within a ~200bp window centered at ~100bp upstream of the transcription start site (TSS), while no significant correlation with responsiveness was detected more than 700bp upstream, or downstream of the TSS or (Figure 1F).

Position specific affinity matrices [PSAMs; (Bussemaker et al., 2007)] provide a more refined representation of DNA binding specificity than simple consensus motifs. We used *MatrixREDUCE* (Foat et al., 2006) to refine the DBE and DAE oligonucleotide motifs into PSAMs that optimally predict DAF-16 responsiveness as proportional to the sum of predicted binding site affinities over all positions within the 700bp upstream promoter region for each gene.

Sequence logo representations of the resulting optimal DBE and DAE matrices are shown in Figure 1G and 1H, along with the enrichment for total promoter affinity in the context of our genomewide DAF-16 target ranking. DBE affinity is significantly enriched in Class I, but not in Class II. DAE affinity is also enriched in Class I, but even more so in Class II gene promoters. We interpret these enrichment patterns as providing strong support for the validity of both our target list and our PSAM representations of DBE and DAE. Our results again indicate that the DBE-binding factor (presumably DAF-16 itself) acts primarily as a transcription activator, while the (unknown) factor that binds to the DAE may activate transcription of Class II targets in *daf-16(−)* conditions.

The transcription factor PQM-1 is strongly associated with DAE affinity

A collection of genomewide *in vivo* binding profiles for 46 transcription factors including DAF-16 was recently generated using whole-animal ChIP-seq profiling of *C. elegans* at various developmental stages (Niu et al., 2011). These data provided us with the opportunity to perform an unbiased search for *trans*-acting factors whose genomic binding sites were enriched for DBE and DAE affinity, respectively, compared to a matching set of control sequences (see Extended Experimental Procedures).

Because we are interested in longevity of adult worms, we focused on the ChIP-seq data for the latest stage available for each factor. As expected, the transcription factor with the highest DBE enrichment was DAF-16 (almost 2-fold, P-value < 10^{-16}; see Figure 2A). The second most enriched factor is PHA-4, a FoxA transcription factor required for Dietary Restriction-mediated longevity (Panowski et al., 2007), which binds to the DBE-related consensus sequence TRTTKRY (R=A/G, K=G/T, Y=C/T).

Unexpectedly, a relatively unknown protein, PQM-1, emerged as the transcription factor whose bound sequences were by far the most enriched in DAE affinity (almost 5-fold; P-value < 10^{-16}; Figure 2B), and much more so than for ELT-3, a GATA transcription factor whose previous implication with aging regulation (Budovskaya et al., 2008) has been under debate (Tonsaker et al., 2012; Zhang et al., 2013). Our observations pointed to PQM-1 as a candidate *trans*-acting factor that recognizes the DAE.

PQM-1 binding sites are enriched upstream of DAF-16 responsive genes

The genomewide ChIP-seq profiles for all tested TFs exhibit a strong peak ~150bp upstream of the transcription start site (Figure 2C), consistent with the expression-based analysis reported in Figure 1F. Accordingly, we assigned a PQM-1 binding site to a gene whenever its center fell between −700 and +100 bp relative to the transcription start site. Using this criterion, 2762 genes were defined as PQM-1 targets. Showing this “regulon” in the context of our DAF-16 responsiveness ranking revealed strong enrichment in both Class I and Class II (Figure 2D and Supplemental Table S4). Notably, in Class II, no fewer than 60% of the 200 top responders have PQM-1 ChIP-seq binding sites in the −700 to +100 bp region of their promoters, compared to a genomewide average of 14%. PQM-1 ChIP-seq targets are enriched in predicted intestinal genes (Figure 2E).

PQM-1 activates transcription through the DAE motif

To directly analyze regulation of gene expression by PQM-1, we used DNA microarrays to assay differential mRNA expression between *pqm-1(ok485)* mutants and wild-type (N2) worms on day 1 of adulthood. We found that both Class I and Class II genes are specifically down-regulated in the *pqm-1* mutant, the largest reduction in expression levels occurring towards the extremes of our ranking (Figure 2F and Supplemental Table S4).

Linear regression, across all genes, of the expression response on the total DAE affinity in the 700bp promoter shows that the presence of DAE binding motifs predicts a reduction in gene expression in the *pqm-1* mutant at a high level of significance ($P < 10^{-16}$; Supplemental Figure S2A).

To confirm that PQM-1 activates gene expression through the DAE, we performed a reporter assay using a representative Class II gene, *F55G11.2*. *pqm-1* is strongly and specifically expressed in the intestine (Reece-Hoyes et al., 2007), a tissue critical for the DAF-16 longevity response (Libina et al. (2003). Consistently, a *pF55G11.2*::*gfp* construct expressed brightly in the intestine (Figure 2G). This GFP expression was reduced considerably by loss of *pqm-1*, as well as by mutation of the DAE motif within the *F55G11.2* promoter (Figure 2H). *pF55G11.2*::*gfp* expression was also reduced in a *daf-2*(−), and increased in a *daf-18/PTEN*(−) background, as expected for a Class II gene (Figure 2I, J). In the absence of *pqm-1*, loss of *daf-2* does not further diminish expression ($P = 0.052$, two-way analysis of variance; Figure 2I). Finally, and importantly, the observed dependency of *pF55G11.2*::*gfp* expression on genetic background is completely lost when the DAE is mutated (Figure 2J).

Together, these data demonstrate that PQM-1 is a *trans*-acting factor that activates transcription though the DAE, and strongly suggest that PQM-1 is a major component of the

DAF-16 transcriptional network, responsible for the downregulation of Class II genes in response to *daf-2* loss.

PQM-1 is required for *daf-2* longevity, development, and dauer recovery

Having established that PQM-1 is a key transcriptional regulator of Class II gene expression, some of which affect longevity (Murphy et al., 2003), we asked whether *daf-2* phenotypes depend on *pqm-1*. First, we tested the effect of *pqm-1* loss-of-function on *daf-2* longevity. Strikingly, reducing PQM-1 activity, either by RNAi or by mutation, shortens the lifespan of *daf-2*(−) animals substantially, by up to 45% (Figure 3A, B; Supplemental Figure S3A, Table S5). This reduction in lifespan is strongly dependent on *daf-2* ($P = 3.4 \times 10^{-8}$ for the interaction between *pqm-1* and *daf-2*, robust Cox Proportional Hazards test, Figure 3B). While this lifespan decrease is milder than is seen after loss of *daf-16*, it exceeds the effect of the loss of individual DAF-16 targets (Murphy et al., 2003), suggesting that PQM-1 activity is a major component of *daf-2*-regulated longevity. *pqm-1* loss also reduces the longevity of the caloric restriction mutant, *eat-2* ($P < 0.0001$, log-rank test; Figure 3C, Supplemental Figure S3C, D, and Supplemental Table S5), suggesting that *pqm-1* is generally required for long life span. Although *pqm-1* mutants have wild-type lifespan (Supplemental Figure 3B), PQM-1::GFP worms, which overexpress the PQM-1 protein, are short-lived compared to wild type (N2) worms (Figure 3A; P<0.0001, log-rank test). Finally, consistent with the role of DAF-16 as an enhancer of stress response, loss of *pqm-1* reduces thermotolerance of *daf-2*(−) worms ($P < 0.001$, log-rank test; Figure 3D and Supplemental Figure S3E).

Examining PQM-1's role in developmental processes, we found that *pqm-1* mutants are only slightly delayed, similar to that observed for *daf-2* mutants and DAF-16 overexpression worms (Supplemental Figure S3F, G); however, *daf-2;pqm-1* double mutants are severely delayed and unsynchronized by 66 hrs post egg-laying ($P = 5 \times 10^{-4}$, Pearson's Chi-Squared Test; Figure 3E). Additionally, when *daf-2* dauers are shifted from the restrictive temperature of 25°C to a permissive temperature of 20°C, loss of *pqm-1* significantly slowed development to adulthood (Figure 3F).

To confirm that PQM-1's subcellular localization is consistent with its observed role in development, we examined larvae containing an integrated PQM-1::GFP translational fusion protein [*unc119(ed3);wgIs201(pqm-1::TY1 EGFP FLAG C;unc119*) (Niu et al., 2011)]. PQM-1 protein is indeed nuclearly localized in all larval stages (Figure 3G), with high abundance particularly from L3 onwards, consistent with an active transcriptional role in development to adulthood and recovery from the dauer stage.

PQM-1 subcellular localization is anti-correlated with that of DAF-16

The mRNA expression level of endogenous *pqm-1* is not considerably changed in *daf-2* or *daf-16* mutants (Shaw et al., 2007), and *Ppqm-1::gfp* worms treated with *daf-2* and *daf-16* RNAi are not obviously different from vector control-treated worms, with high levels of expression in the intestine all three conditions (Supplemental Figure S4A). Thus, IIS regulation of PQM-1 is unlikely to occur at the transcriptional level.

The degree to which DAF-16 activates gene expression is modulated primarily through post-translational regulation of its subcellular localization by the insulin/IGF-1 signaling (IIS) pathway (Lin et al., 2001; Ogg et al., 1997). To test whether IIS regulates PQM-1 post-transcriptionally in a similar manner, we quantified the nuclear and cytoplasmic localization of DAF-16::GFP and PQM-1::GFP under varying conditions (Berdichevsky et al., 2006; Henderson and Johnson, 2001; Hertweck et al., 2004; Wolff et al., 2006); see Experimental Procedures for details). Representative images are shown in Figure 4A. We found that the

nuclear localization of PQM-1::GFP was strongly dependent on IIS (Figure 4C, Supplemental Table S6). Significantly, however, it was the opposite of that of DAF-16 (Figure 4B): while PQM-1 was mostly (~80%) nuclearly localized under normal conditions, it became more cytoplasmic under *daf-2(−)* conditions, when DAF-16 by contrast became strongly nuclear. Conversely, under *daf-18/PTEN(−)* conditions, when DAF-16 was cytoplasmic, PQM-1 remained nuclearly localized (Figure 4B,C). Reduction of the 14-3-3 protein *par-5* slightly shifted PQM-1::GFP out of the nucleus (Figure 4A,C), which is also the opposite of its effect on DAF-16 (Figure 4A,B) (Berdichevsky et al., 2006). Together, these data suggest that the IIS pathway controls the subcellular localization of PQM-1 and DAF-16 in opposite ways.

Stress conditions also affected PQM-1's subcellular localization. In particular, heat treatment, which drives DAF-16 into the nucleus (Figure 4D,E), shifted PQM-1 out of the nucleus (Figure 4D,F). We also studied the dynamics of PQM-1::GFP and DAF-16::GFP translocation during the response to heat treatment (35°C) and the subsequent recovery from this stress (20°C). Upon heat stress, DAF-16 enters the nucleus, while PQM-1 leaves it (Figure 4G). After the worms were shifted back to 20°C, the proteins returned to their original respective locations at similar rates (Figure 4H). Thus, the two proteins populate opposite subcellular compartments, as a function of time as well as the level of insulin/IGF-1 signaling.

Nuclear localization of DAF-16 and PQM-1 is mutually antagonistic

Because DAF-16 only seems to directly control Class I gene expression, effect of *daf-16* loss on Class II gene expression is unexplained, given the definition of Class I and II in terms of differential expression between *daf-2(−)* and *daf-2(−);daf-16(−)* worms. This motivated us to investigate whether PQM-1 and DAF-16 influence each other's subcellular localization (Figure 5A–D). In an otherwise wild-type animal, loss of *pqm-1* partially shifts DAF-16::GFP to the nucleus ($P = 1.5 \times 10^{-3}$, Pearson Chi-Squared Test; Figure 5C), while loss of *daf-16* has no observable effect on PQM-1::GFP localization ($P = 0.89$; Figure 5D). Strikingly, in *daf-2* mutants, where DAF-16::GFP is strongly nuclear (Figure 4A), RNAi knockdown of *daf-16* significantly shifted PQM-1::GFP from the cytoplasm to the nucleus ($P = 0.002$; Figure 5B,D). This suggests an indirect mechanism by which loss of *daf-16* in a *daf-2* background would cause an increase in Class II expression (Figure 5E).

Together, these data suggest that DAF-16 and PQM-1 antagonize each other with regard to localization in the nucleus, providing the cell with an elegant mechanism for switching between a stress-reponsive state (in which DAF-16 is nuclear and activates Class I genes) and a growth-enabling state (in which PQM-1 is nuclear and primarily activates Class II genes). The position of the switch is determined by the signaling status of the IIS pathway (Figure 5E)

Expression of DAF-16-responsive genes decreases with age

The intimate connection between IIS and longevity motivated us to examine the role that DAF-16 targets might play in wild-type aging. The 1255 genes previously identified as regulated with age in wild-type *C. elegans* (Budovskaya et al., 2008) are also highly enriched in Class I and Class II genes (Figure 6A, Supplemental Table S4). Analyzing genomewide mRNA expression data from the same study, we observed a progressive decrease with age in the average expression of both Class I and Class II (Figure 6B, C). This suggests a significant role for DAF-16 targets in normal aging.

Loss of PQM-1 activity underlies expression loss over normal lifespan

Our observation that PQM-1 is required for the extended longevity and stress response of *daf-2* mutants led us to wonder whether its transcriptional activity and localization change with age. Indeed, we found that PQM-1 is the transcription factor whose ChIP-seq binding sites are the most enriched in the upstream regions of the genes most downregulated with age (Figure 6D). Moreover, the progressive decrease with age in the average expression of the PQM-1 regulon (defined as above) exceeds that of any other surveyed transcription factor (Figure 6E). Consistent with this observation, when we compared animals on Day 1 and Day 7, we found that both PQM-1::GFP and DAF-16::GFP become increasingly cytoplasmic with age. PQM-1's shift from 80% nuclear to 90% cytoplasmic is particularly striking (Figure 6F–H). Together, these data suggest that a major fraction of age-related transcriptional changes could be caused by loss of nuclear PQM-1.

DISCUSSION

We have revealed an unexpected and major role for the little-studied transcription factor PQM-1 in longevity, development, and stress response regulation. Our data suggest that PQM-1 is a core component of a heretofore unknown *trans*-acting factor that complements DAF-16/FOXO in multiple respects.

The starting point for our study was our novel voting algorithm for ranking *C. elegans* genes according to their DAF-16 responsiveness, which we applied to 75 genomewide expression profiles from five different studies (McElwee et al., 2003; McElwee et al., 2004; Murphy et al., 2003; Shaw et al., 2007; Troemel et al., 2006). This not only allowed us to verify previous DAF-16 targets and identify new ones, but most importantly, to uncover PQM-1 as the transcription factor by far the most strongly associated with the DAF-16 associated element (DAE).

PQM-1 activates gene expression through the DAE

Our identification of PQM-1 as a plausible DAE binding factor resolves an outstanding issue raised by previous DAF-16 transcriptional studies, which had suggested that another factor than DAF-16 might bind the DAE (Murphy et al., 2003; Schuster et al., 2010). The DAE consensus (TGATAAG / CTTATCA) has more similarity to a GATA motif than to the forkhead consensus (TGTTTAC / GTAAACA). This indicated that the DAE was unlikely to be bound by DAF-16 itself, but rather should be bound by a separate factor.

The GATA-binding factor ELT-3 was hypothesized to bind the DAE, to regulate transcriptional changes with age, and to contribute to longevity through its activity in the intestine (Budovskaya et al., 2008). These observations, however, have recently been questioned due to ELT-3's lack of expression in intestinal tissue and inconsistent longevity effects (Tonsaker et al., 2012). Another recent study suggests that ELT-3 and ELT-2, another GATA factor, may act as hypodermis- and intestine-specific co-activators of DAF-16 Class I targets, respectively, but are not regulators of Class II genes (Zhang et al., 2013). Our analysis revealed that ELT-3 is significantly less enriched for the DAE in its ChIP-seq binding sites than is PQM-1 (Figure 2B). Furthermore, ELT-3 targets, as defined by ChIP-seq, show significantly less age-dependent transcriptional change than do PQM-1 targets (Figure 6E). PQM-1 is highly expressed in the intestine, where Class II targets are most likely to be expressed, and its nuclear localization declines with age (Figure 6F, G), consistent with the declining expression of its predicted targets.

Alic, et al. recently performed genomewide expression profiling of the contrast between *Drosophila InR* and *InR;dfoxo* genotypes, analogous to the contrast between *daf-2* and *daf-16;daf-2* in *C. elegans* (Alic et al., 2011). They concluded that *dFOXO* only directly

activates genes, and that an unknown factor, likely one that binds to a GATA-containing motif, must be responsible for the *dfoxo*-dependent but indirect downregulation of gene expression in IIS mutants. In addition, a significant overlap was found between the genes downregulated indirectly by *dfoxo* and the Class II genes in Murphy et al. (2003). This complements our own results in a striking manner, and strongly suggests that PQM-1 has a functional homolog in *Drosophila*.

PQM-1 is a relatively uncharacterized transcription factor. Knowledge about its function so far has been limited to its upregulated expression upon paraquat treatment (Tawe et al., 1998) and *Pseudomonas* infection (Shapira et al., 2006), its requirement for *Pseudomonas* infection survival (Shapira et al., 2006), and its expression in the intestine (Reece-Hoyes et al., 2007).

Phylogenetic analysis suggests that the PQM-1 protein belongs to the family of BTB-ZF transcription factors (M. Huynen, personal communication), whose members combine an N-terminal BTB/POZ domain that mediates protein-protein interactions with a C-terminal C2H2 Zinc finger (ZF) domain that mediates sequence-specific DNA interactions, and have been implicated with lymphopoietic and neurological development as well as regulation of fertility (Siggs and Beutler, 2012). The human genome encodes 49 BTB-ZF genes, including the B cell development master regulator Bcl6 (Siggs and Beutler, 2012). Taken together, these facts suggest that PQM-1's role in the regulation of growth and development, like that of DAF-16/FOXO in stress response, may be evolutionarily conserved.

An integrated model of DAF-16 and PQM-1 activity and regulation

Our data support a cis-regulatory model in which both the DBE and the DAE contribute to the expression regulation of Class I genes (Supplemental Figure S2B), while Class II genes are exclusively controlled through the DAE (Figure 1G,H). Under normal conditions, the DAE-dependent transcriptional activation of Class II genes by nuclear PQM-1 enables growth and development, while a modest activation of Class I genes allows mild stresses to be combatted while the organism develops. Upon acute stress, growth and development must be arrested while the organism fully activates its stress responses. To achieve this, PQM-1 leaves the nucleus while DAF-16 enters. The nuclear exit of PQM-1 causes expression of Class II genes to fall in response to loss of activation through the DAE; at the same time, DAF-16 moves into the nucleus, where its binding to the DBE in the upstream promoter region of Class I genes more than compensates for the loss of activation by PQM-1, giving rise to a net increase in Class I expression.

While DAF-16 and PQM-1 seem to act independently in activating their transcriptional targets, their respective subcellular localizations are strongly interdependent. First, we found that PQM-1 nuclear localization is anti-correlated with the nuclear localization of DAF-16 when the activity of the IIS pathway is varied (Figure 4). Second, beyond the anti-correlated behavior in response to changes in IIS activity, we discovered an active mutual antagonism between nuclear DAF-16 and nuclear PQM-1 (Figure 5). In particular, nuclear DAF-16 seems to contribute to the nuclear exclusion of PQM-1, as *daf-16* loss of function, in conditions where DAF-16 is nuclear, leads to (partial) nuclear re-entry of PQM-1 (Figure 5D). This is a crucial finding, as it explains how loss of *daf-16* in a *daf-2(−)* background activates Class II genes. Had IIS controlled PQM-1 localization solely in a *daf-16*-independent manner, this would have left the difference in Class II gene expression between *daf-2(−)* and *daf-16(−);daf-2(−)* unaccounted for, since DAF-16 seems to only control Class I genes directly.

Our characterization of PQM-1 has revealed an elegant mechanism for carefully tuning the physiologically important balance between stress response and development (Figure 5E).

While stress response is required for survival of an acute insult, such a state may be energetically costly to maintain or may be deleterious for development. For example, overexpression of DAF-16 (Libina et al., 2003) and HSF-1 (Hsu et al., 2003), as well as *daf-2* deletion, which induces strong DAF-16 nuclear localization, causes developmental delays, arrest, and embryonic lethality. By contrast, inducing the activity of these factors late in life improves longevity. Through its antagonism with DAF-16, nuclear presence of PQM-1 could help the worm maintain an "unstressed" transcriptional state that may be critical to the animal's ability to develop. Indeed, many of PQM-1's transcriptional targets are associated with growth and development (Supplemental Table S7), and novel DAF-16 Class II (downregulated) targets are associated with GO terms that suggest that DAF-16 activity is a negative regulator of growth and development to reproduction, consistent with the reduction of development rates upon DAF-16 overexpression [Supplemental Figure S3F and (Kawasaki et al., 2010)]. While this model requires further validation, our findings suggest that the ability of an organism to mount a stress response and to recover from stress response when it is no longer needed are both important aspects of survival as well as growth and development. PQM-1 is a crucial new component of this important regulatory mechanism.

In spite of this progress, our study leaves several questions unanswered. For instance, the molecular mechanisms through which PQM-1 localization depends on insulin/IGF-1 signaling status – directly and/or via competition for nuclear localization with DAF-16 – remain to be elucidated. Furthermore, we do not currently have a good explanation why loss of *pqm-1* in a *daf-2(−)* background reduces lifespan, rather than extending it. A modest reduction of Class II gene expression due to the loss of residual nuclear PQM-1 might be expected to lead to further extension of lifespan, inconsistent with our observations. Perhaps it is the loss of the low-level activating contribution of PQM-1 to Class I genes via the DAE, which leads to a reduction in stress response, that causes shortened lifespan. Further study will be required to resolve these issues.

Loss of nuclear PQM-1 during natural aging: cause or consequence?

Taken together, our data strongly suggest that a progressive loss of nuclear PQM-1 causes the expression of both Class I and II genes to decrease with age (Figure 6). In *daf-2* mutants, the changes in Class I and II gene expression are in opposite directions, both of which benefits survival, be it in complementary ways. In aging wild-type worms, expression of both Class I and Class II genes is reduced, and the net effect on survival is less obvious. It also remains an open question whether this loss of nuclear PQM-1 is a cause or a consequence of aging. One possibility is that loss of nuclear PQM-1 is a response to stress caused by unknown drivers of aging; DAF-16 however leaves the nucleus with age, rather than entering it. Alternatively, PQM-1 itself could be one of those drivers. Providing an answer to this question would deepen our understanding of the mechanisms underlying natural aging.

EXPERIMENTAL PROCEDURES

Microarray reanalysis and voting algorithm

We re-analyzed raw genomewide expression data from five studies (McElwee et al., 2003; McElwee et al., 2004; Murphy et al., 2003; Shaw et al., 2007; Troemel et al., 2006) encompassing 75 genomewide expression profiles, which we used to construct 46 explicit contrasts between conditions with differing levels of DAF-16 activity. After complete reprocessing of the raw data (array-specific standardization, normalization, and re-mapping of probes), a log-fold-change and corresponding standard error were calculated for each transcript on each array (or array pair for single-channel technologies). Together, these were

converted into a "vote" value between −1 (highly likely to be downregulated) and +1 (highly likely to be upregulated). The total voting score for each gene was computed as the sum of voting scores for individual experiments, which is robust in the sense that the influence of any individual experiment is limited to a single full vote. An empirical null distribution based on random permutation was created, and all genes were ranked from consistently upregulated (Class I) to consistently downregulated (Class II). The area under the null distribution (p-value) for each gene that served as the basis for assigning genes to Class I or Class II at a 5% false discovery rate. For details see Extended Experimental Procedures.

C. elegans genetics

All strains were cultured using standard methods (Brenner, 1974). In all experiments, N2 is wild type. LG II: *pqm-1(ok485)*. LG III: *daf-2(e1370)*.

Strains

OP201 (*unc119(ed3);wgIs201(pqm-1::TY1 EGFP FLAG C;unc119)*); UL1735 (*Ppqm-1::gfp*); CQ200 (*pqm-1(ok485*);*daf-2(e1370)*); RB711 *(pqm-1(ok485)*; CQ254 (6x outcrossed *pqm-1(ok485)*); CF1041 (*daf-2(e1370)*); CQ201 (*pF55G11.2(wt DAE)::gfp*); CQ204 (*pqm-1; pF55G11.2(wt DAE)::gfp*); CQ202 (*pF55G11.2(mut DAE)::gfp*).

DAE reporter strain construction

700 bp upstream of the *F55G11.2* translational start site was cloned into the pPD95.75::GFP Fire expression vector. N2 animals were injected with *pF55G11.2::GFP* at 25 ng/μl and 1 ng/μl *Pmyo3::mCherry* as a coinjection marker, then crossed into *pqm-1* animals. The DAE consensus sequence at 115 bp upstream of the translational start site (GTTATCA) was mutated to GTgggCA using Quikchange mutagenesis (Agilent) and subcloned into pPD95.75::GFP. N2 animals were injected as described for the wt promoter.

RNAi strains

Other than pAD12 (vector control), pAD48 (*daf-2*), and pAD43 (*daf-16*) (Dillin et al., 2002), all RNAi clones were obtained from the Ahringer RNAi collection (Fraser et al., 2000) and sequence verified.

Microarray analysis

RNA was extracted from *pqm-1(ok485)* and N2 worms, cRNA was linearly amplified, Cy3/Cy5 labeled, hybridized to the Agilent 44k *C. elegans* microarray, and analyzed as previously described (Shaw et al., 2007).

Survival analysis

Day 1 of adulthood was defined as t=0, and the log-rank (Mantel-Cox) method was used to test the null hypothesis in Kaplan-Meier survival analysis (Lawless, 1982), and evaluated using OASIS survival analysis software (Yang et al., 2011). The log cumulative hazard function was also estimated (Supplemental Information). All experiments were carried out at 20°C; n ≥ 60 per strain/trial.

Thermotolerance assay

Worms were grown at 20°C on OP50. On Day 1 of adulthood, n ≥ 60 were picked onto pre-warmed plates and placed at 35°C, then scored hourly.

Developmental assay

Worms were grown at 20°C and bleached to developmentally synchronize. n > 100 were scored for developmental stage.

Dauer recovery assay

daf-2(e1370) eggs were incubated at 25°C to induce dauer formation; ~240 dauers were picked/strain (10 dauers/well of 24-well NGM plate with either L4440 vector control or *pqm-1(RNAi)*) at 20°C, then photographed at 20× (SMZ1500) over three days, and compared with dauer and adult controls (Matlab); size distribution differences were compared using the Mann-Whitney U test (see Expanded Experimental Procedures).

DAF-16::GFP and PQM-1::GFP localization assays

Each strain was grown at 20°C then bleached onto RNAi bacteria; 20–50 animals were imaged at 10× and 40× and scored blindly for nuclear, cytoplasmic, and diffuse localization (Berdichevsky et al., 2006; Henderson and Johnson, 2001; Hertweck et al., 2004; Wolff et al., 2006). Because each animal showed consistent cell-to-cell localization of DAF-16 and PQM-1, each was scored as one point. SEP for each sample is shown; comparison P-values were calculated using Pearson's chi-squared test.

Heat stress and recovery

DAF-16::GFP and PQM-1::GFP worms were imaged after shifting to 35°C and also after shifting back to 20°C, then scored for nuclear, cytoplasmic, and diffuse localization.

Supplementary Material

Refer to Web version on PubMed Central for supplementary material.

Acknowledgments

We thank the *C. elegans* Genetics Center, I. Hope, and S. Kim for strains, X.-J. Lu for implementing the REDUCE suite, M. Huynen for help with the phylogenetic analysis of the PQM-1 protein sequence, M. Chalfie, I. Greenwald, O. Hobert, and members of the Bussemaker and Murphy laboratories, and the anonymous reviewers for valuable suggestions. This work was supported by NIH grants R01HG003008, U54CA121852, and P50GM071508, as well as a John Simon Guggenheim Foundation Fellowship to HJB, and by NIH Innovator award DP2OD004402 and R01AG034446 and grants from the Glenn and Keck Foundations to CTM.

REFERENCES

Alic N, Andrews TD, Giannakou ME, Papatheodorou I, Slack C, Hoddinott MP, Cocheme HM, Schuster EF, Thornton JM, Partridge L. Genome-wide dFOXO targets and topology of the transcriptomic response to stress and insulin signalling. Molecular systems biology. 2011; 7:502. [PubMed: 21694719]

Berdichevsky A, Viswanathan M, Horvitz HR, Guarente L. C. elegans SIR-2.1 interacts with 14-3-3 proteins to activate DAF-16 and extend life span. Cell. 2006; 125:1165–1177. [PubMed: 16777605]

Boorsma A, Lu XJ, Zakrzewska A, Klis FM, Bussemaker HJ. Inferring condition-specific modulation of transcription factor activity in yeast through regulon-based analysis of genomewide expression. PloS one. 2008; 3:e3112. [PubMed: 18769540]

Brenner S. The genetics of *Caenorhabditis elegans*. Genetics. 1974; 77:71–94. [PubMed: 4366476]

Budovskaya YV, Wu K, Southworth LK, Jiang M, Tedesco P, Johnson TE, Kim SK. An elt-3/elt-5/elt-6 GATA transcription circuit guides aging in C. elegans. Cell. 2008; 134:291–303. [PubMed: 18662544]

Bussemaker HJ, Foat BC, Ward LD. Predictive modeling of genome-wide mRNA expression: from modules to molecules. Annual review of biophysics and biomolecular structure. 2007; 36:329–347.

Chikina MD, Huttenhower C, Murphy CT, Troyanskaya OG. Global prediction of tissue-specific gene expression and context-dependent gene networks in Caenorhabditis elegans. PLoS computational biology. 2009; 5:e1000417. [PubMed: 19543383]

Dillin A, Crawford DK, Kenyon C. Timing requirements for insulin/IGF-1 signaling in *C. elegans*. Science. 2002; 298:830–834. [PubMed: 12399591]

Dong MQ, Venable JD, Au N, Xu T, Park SK, Cociorva D, Johnson JR, Dillin A, Yates JR 3rd. Quantitative mass spectrometry identifies insulin signaling targets in C. elegans. Science. 2007; 317:660–663. [PubMed: 17673661]

Foat BC, Morozov AV, Bussemaker HJ. Statistical mechanical modeling of genome-wide transcription factor occupancy data by MatrixREDUCE. Bioinformatics. 2006; 22:e141–149. [PubMed: 16873464]

Fraser AG, Kamath RS, Zipperlen P, Martinez-Campos M, Sohrmann M, Ahringer J. Functional genomic analysis of *C. elegans* chromosome I by systematic RNA interference. Nature. 2000; 408:325–330. [PubMed: 11099033]

Furuyama T, Nakazawa T, Nakano I, Mori N. Identification of the differential distribution patterns of mRNAs and consensus binding sequences for mouse DAF-16 homologues. Biochem J. 2000; 349:629–634. [PubMed: 10880363]

Halaschek-Wiener J, Khattra JS, McKay S, Pouzyrev A, Stott JM, Yang GS, Holt RA, Jones SJ, Marra MA, Brooks-Wilson AR, et al. Analysis of long-lived C. elegans daf-2 mutants using serial analysis of gene expression. Genome Res. 2005; 15:603–615. [PubMed: 15837805]

Henderson ST, Johnson TE. *daf-16* integrates developmental and environmental inputs to mediate aging in the nematode *Caenorhabditis elegans*. Curr Biol. 2001; 11:1975–1980. [PubMed: 11747825]

Hertweck M, Gobel C, Baumeister R. C. elegans SGK-1 is the critical component in the Akt/PKB kinase complex to control stress response and life span. Dev Cell. 2004; 6:577–588. [PubMed: 15068796]

Honda Y, Honda S. The *daf-2* gene network for longevity regulates oxidative stress resistance and Mn-superoxide dismutase gene expression in *Caenorhabditis elegans*. Faseb J. 1999; 13:1385–1393. [PubMed: 10428762]

Hsu AL, Murphy CT, Kenyon C. Regulation of aging and age-related disease by DAF-16 and heat-shock factor. Science. 2003; 300:1142–1145. [PubMed: 12750521]

Kawasaki I, Jeong MH, Oh BK, Shim YH. Apigenin inhibits larval growth of Caenorhabditis elegans through DAF-16 activation. FEBS letters. 2010; 584:3587–3591. [PubMed: 20647014]

Kenyon C. The plasticity of aging: insights from long-lived mutants. Cell. 2005; 120:449–460. [PubMed: 15734678]

Kenyon C, Chang J, Gensch E, Rudner A, Tabtiang R. A *C. elegans* mutant that lives twice as long as wild type. Nature. 1993; 366:461–464. [PubMed: 8247153]

Lawless, JF. Models and Methods for Lifetime Data. Wiley; New York: 1982.

Lee SS, Kennedy S, Tolonen AC, Ruvkun G. DAF-16 target genes that control C. elegans life-span and metabolism. Science. 2003; 300:644–647. [PubMed: 12690206]

Libina N, Berman JR, Kenyon C. Tissue-specific activities of C. elegans DAF-16 in the regulation of lifespan. Cell. 2003; 115:489–502. [PubMed: 14622602]

Lin K, Dorman JB, Rodan A, Kenyon C. *daf-16*: An HNF-3/forkhead family member that can function to double the life-span of *Caenorhabditis elegans*. Science. 1997; 278:1319–1322. [PubMed: 9360933]

Lin K, Hsin H, Libina N, Kenyon C. Regulation of the *Caenorhabditis elegans* longevity protein DAF-16 by insulin/IGF-1 and germline signaling. Nature genetics. 2001; 28:139–145. [PubMed: 11381260]

McElwee J, Bubb K, Thomas JH. Transcriptional outputs of the Caenorhabditis elegans forkhead protein DAF-16. Aging Cell. 2003; 2:111–121. [PubMed: 12882324]

McElwee JJ, Schuster E, Blanc E, Thomas JH, Gems D. Shared transcriptional signature in Caenorhabditis elegans Dauer larvae and long-lived daf-2 mutants implicates detoxification system in longevity assurance. J Biol Chem. 2004; 279:44533–44543. [PubMed: 15308663]

Murphy, CT. Exp Gerontol. 2006. The search for DAF-16/FOXO transcriptional targets: Approaches and discoveries.

Murphy CT, Kenyon C. Enrichment of regulatory motifs upstream of predicted DAF-16 targets. Nature genetics. 2006; 38:397–398. [PubMed: 16570056]

Murphy CT, McCarroll SA, Bargmann CI, Fraser A, Kamath RS, Ahringer J, Li H, Kenyon C. Genes that act downstream of DAF-16 to influence the lifespan of Caenorhabditis elegans. Nature. 2003; 424:277–283. [PubMed: 12845331]

Niu W, Lu ZJ, Zhong M, Sarov M, Murray JI, Brdlik CM, Janette J, Chen C, Alves P, Preston E, et al. Diverse transcription factor binding features revealed by genome-wide ChIP-seq in C. elegans. Genome Res. 2011; 21:245–254. [PubMed: 21177963]

Ogg S, Paradis S, Gottlieb S, Patterson GI, Lee L, Tissenbaum HA, Ruvkun G. The Fork head transcription factor DAF-16 transduces insulin-like metabolic and longevity signals in *C. elegans*. Nature. 1997; 389:994–999. [PubMed: 9353126]

Oh SW, Mukhopadhyay A, Dixit BL, Raha T, Green MR, Tissenbaum HA. Identification of direct DAF-16 targets controlling longevity, metabolism and diapause by chromatin immunoprecipitation. Nature genetics. 2006; 38:251–257. [PubMed: 16380712]

Panowski SH, Wolff S, Aguilaniu H, Durieux J, Dillin A. PHA-4/Foxa mediates diet-restriction-induced longevity of C. elegans. Nature. 2007; 447:550–555. [PubMed: 17476212]

Reece-Hoyes JS, Shingles J, Dupuy D, Grove CA, Walhout AJ, Vidal M, Hope IA. Insight into transcription factor gene duplication from Caenorhabditis elegans Promoterome-driven expression patterns. BMC genomics. 2007; 8:27. [PubMed: 17244357]

Schuster E, McElwee JJ, Tullet JM, Doonan R, Matthijssens F, Reece-Hoyes JS, Hope IA, Vanfleteren JR, Thornton JM, Gems D. DamID in C. elegans reveals longevity-associated targets of DAF-16/FoxO. Molecular systems biology. 2010; 6:399. [PubMed: 20706209]

Shapira M, Hamlin BJ, Rong J, Chen K, Ronen M, Tan MW. A conserved role for a GATA transcription factor in regulating epithelial innate immune responses. Proc Natl Acad Sci U S A. 2006; 103:14086–14091. [PubMed: 16968778]

Shaw WM, Luo S, Landis J, Ashraf J, Murphy CT. The C. elegans TGF-beta Dauer pathway regulates longevity via insulin signaling. Curr Biol. 2007; 17:1635–1645. [PubMed: 17900898]

Siggs OM, Beutler B. The BTB-ZF transcription factors. Cell Cycle. 2012; 11:3358–3369. [PubMed: 22894929]

Tawe WN, Eschbach ML, Walter RD, Henkle-Duhrsen K. Identification of stress-responsive genes in Caenorhabditis elegans using RT-PCR differential display. Nucleic Acids Res. 1998; 26:1621–1627. [PubMed: 9512531]

Tonsaker T, Pratt RM, McGhee JD. Re-evaluating the role of ELT-3 in a GATA transcription factor circuit proposed to guide aging in C. elegans. Mechanisms of ageing and development. 2012; 133:50–53. [PubMed: 22001047]

Troemel ER, Chu SW, Reinke V, Lee SS, Ausubel FM, Kim DH. p38 MAPK regulates expression of immune response genes and contributes to longevity in C. elegans. PLoS genetics. 2006; 2:e183. [PubMed: 17096597]

Wolff S, Ma H, Burch D, Maciel GA, Hunter T, Dillin A. SMK-1, an essential regulator of DAF-16-mediated longevity. Cell. 2006; 124:1039–1053. [PubMed: 16530049]

Yang JS, Nam HJ, Seo M, Han SK, Choi Y, Nam HG, Lee SJ, Kim S. OASIS: online application for the survival analysis of lifespan assays performed in aging research. PloS one. 2011; 6:e23525. [PubMed: 21858155]

Zhang P, Judy M, Lee SJ, Kenyon C. Direct and Indirect Gene Regulation by a Life-Extending FOXO Protein in C. elegans: Roles for GATA Factors and Lipid Gene Regulators. Cell metabolism. 2013; 17:85–100. [PubMed: 23312285]

Research Highlights

1. DAF-16 only activates gene expression, through the DAF-16 binding element (DBE)
2. PQM-1 activates gene expression through the DAF-16 associated element (DAE)
3. PQM-1 and DAF-16 are nuclear in opposite IIS conditions and are mutually antagonistic
4. PQM-1 exits the nucleus in old age, causing the expression of its targets to decline

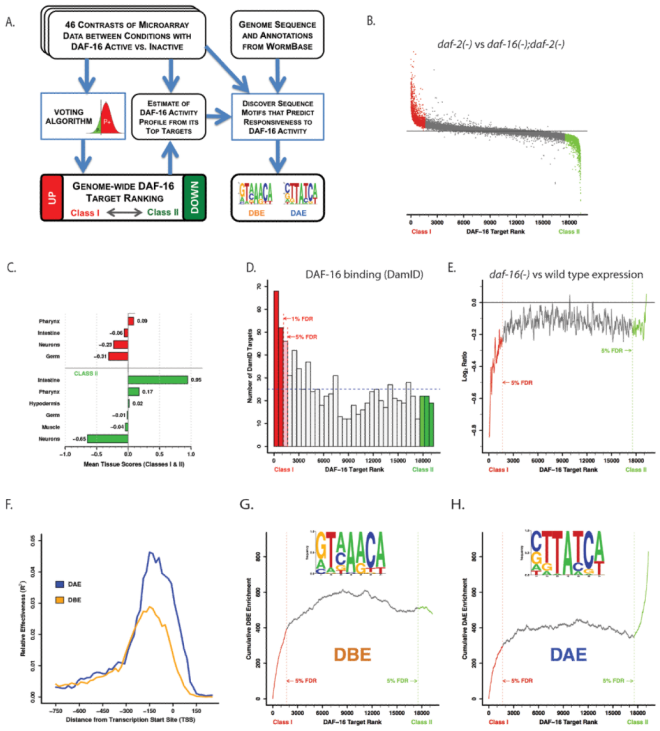

FIGURE 1. A new DAF-16-responsiveness ranking algorithm highlights a missing regulator of *daf-2* gene expression

A. Schematic diagram illustrating the voting algorithm we developed to integrate differential expression data from a large number of studies. At a 5% false discovery rate (FDR), we classified as 1663 positive (Class I) and 1733 negative (Class II) DAF-16 targets. Class I genes are enriched for the Gene Ontology categories of oxidation, reduction, and energy metabolism, while Class II genes are enriched for biosynthesis, growth, reproduction, and development.

B. Log_2-ratio of *daf-2(−)* vs *daf-16(−);daf-2(−)* conditions averaged over all 46 contrasts, with genes shown in order of DAF-16 responsiveness.

C. Class I targets are enriched for predicted hypodermal genes and depleted for neuronal genes, while Class II targets are strongly enriched for intestinal genes.

D. Visualization in the context of our ranking of the set of genes previously defined as DAF-16 targets based in vivo genomic binding profile obtained using DamID (Schuster et al., 2010), confirming the association of DAF-16 binding with positive (but not with negative) response to DAF-16 activation.

E. Differential mRNA expression between an N2 reference strain and a *daf-16* mutant (Budovskaya et al., 2008) in the context of our ranking.

F. Effectiveness of DBE and DAE affinity as a predictor of responsiveness to DAF-16 activation, quantified as the coefficient of determination (R^2) associated with a sliding 200bp sequence window.

G. Plot of cumulative DBE affinity in excess of its genomewide expected value, shown in the context of our ranking in terms of DAF-16 responsiveness, showing that the DBE is primarily associated with Class I genes.

H. Idem for DAE affinity, showing that it is associated both with Class I and with Class II genes.

See also Supplemental Figure S1 and Supplemental Table S2 and S4

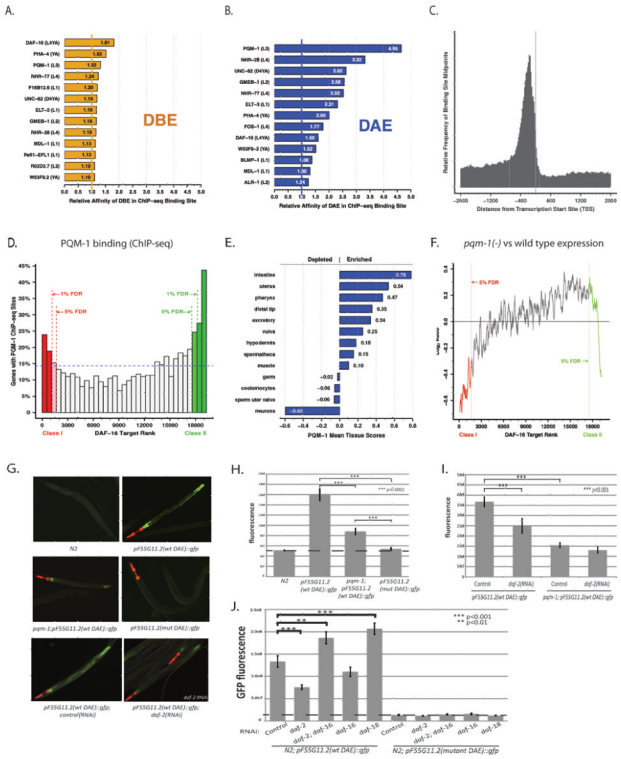

FIGURE 2. PQM-1 is the DAE-binding factor

A. Fold-enrichment over random expectation of DBE affinity in sequences bound by each of the 46 transcription factors assayed by the modENCODE consortium using ChIP-seq (Niu et al., 2011); the last stage assayed was analyzed. Shown are the 13 most highly enriched factors ($P < 10^{-16}$ in each case; see Extended Experimental Procedures). As expected, the highest enrichment is found in DAF-16-bound regions.

B. Same as **A**, but for DAE affinity. The latter is strikingly enriched within sequences bound by PQM-1.

C. Distribution of ChIP-seq binding site centers relative to transcriptional start sites, based on all modENCODE ChIP-seq data (Niu et al., 2011).

D. PQM-1 binding sites are significantly enriched upstream of both Class I and Class II genes, with the strongest effect for Class II.

E. PQM-1 targets are predicted to primarily be intestinally expressed, and depleted in neurons.

F. Both Class I and Class II genes are specifically downregulated in the *pqm-1* mutant relative to wild type.

G–J. A promoter-GFP construct of a PQM-1-regulated Class II gene, *F55G11.2*, that contains a DAE motif in its promoter is abundantly expressed in the intestine of wild-type worms, but its expression is decreased in the *pqm-1(−)* background ($P < 0.0001$, Student's *t*-test for unpaired samples), when the DAE is mutated ($P < 0.001$) (**H, I, J**), and in a *daf-2* background (**I, J**), and is increased in a *daf-18/PTEN* background in a DAE-dependent manner (**J**).

See also Supplemental Table S4 and S6 and Figure S2.

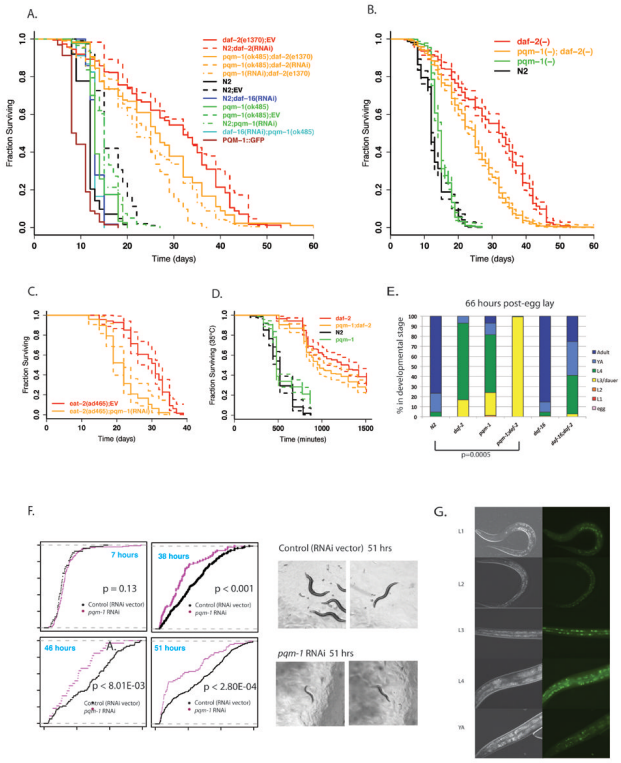

FIGURE 3. PQM-1 is required for normal development and longevity

A. Survival curves for various conditions. Loss of *pqm-1* partially suppresses the life span extension of *daf-2* mutants (red vs. orange lines; p<0.0001), while *pqm-1(−)* has no significant effect on N2 (wild type; black vs. green lines) or *daf-16* life spans (blue vs aqua), while overexpression of PQM-1 (brown) shortens life span. See Supplemental Figure S3A for log-mortality plots and Supplemental Table S5 for additional statistics.

B. A subset of the same data, pooled by genotype, showing the genetic epistasis between *daf-2* and *pqm-1* ($P = 3.4 \times 10^{-8}$, robust Cox Proportional Hazards test).

C. *pqm-1* is required for *eat-2*s long life span (31 days vs. 22 days at 50% mortality, Bonferroni p-value <0.0001).

D. *pqm-1(−)* reduces *daf-2's* thermotolerance ($P = 0.0003$; Supplemental Table S5).

E. Development of *daf-2;pqm-1* double mutants is severely delayed by 66 hours post-hatching (see Supplemental Figure S3F for time course).

F. Loss of *pqm-1* slows recovery of *daf-2* dauers after temperature shift (25 to 20°C). Size distributions are shown for each strain as empirical cumulative distributions, and compared using the Mann-Whitney U test. On day 1 (7 hours after shift), size distributions were indistinguishable (see Supplemental Table S5 for details). By 38 hours, *pqm-1* loss significantly slows development. *daf-2* worms after 51 hours are significantly smaller on *pqm-1* RNAi than on control RNAi (same magnification).

G. PQM-1 protein localizes to intestinal nuclei, becoming very visible at L3 and persisting into adulthood.

See also Supplemental Table S5 and Figure S3.

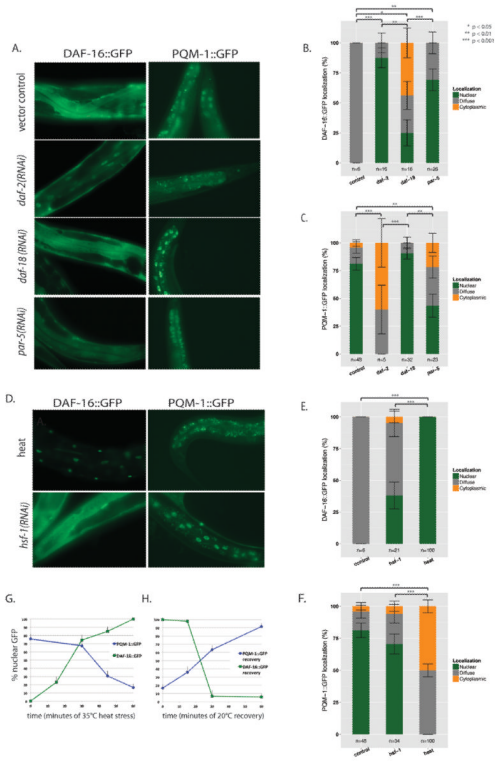

FIGURE 4. IIS and heat regulation of PQM-1 localization

Animals were scored for nuclear, cytoplasmic, and diffuse localization. (**A**) Representative images for each sample; DAF-16::GFP is driven into the nucleus under *daf-2(−)* and *par-5(−),*conditions, and becomes cytoplasmic under *daf-18/PTEN(−)* conditions (**B**); PQM-1::GFP, by contrast, is mostly nuclear under normal conditions, cytoplasmic with *daf-2(RNAi),* and nuclear with *daf-18(RNAi)* (**C**), suggesting that DAF-16 and PQM-1 are regulated by the IIS pathway in opposite directions.

D–F. Upon heat shock (35°C for 1 hour), DAF-16::GFP becomes nuclearly localized (E), while PQM-1 moves to the cytoplasm (F).

G, H: PQM-1 and DAF-16 display opposite patterns of nuclear localization upon heat stress (35°C; **G**) and recovery (20°C; **H**).

Pairwise distribution comparison P-values here and in Figures 5 and 6 were calculated using Pearson's chi-squared test with a sampled null distribution. Only a subset of these are shown here; full results can be found in Supplemental Table S6.

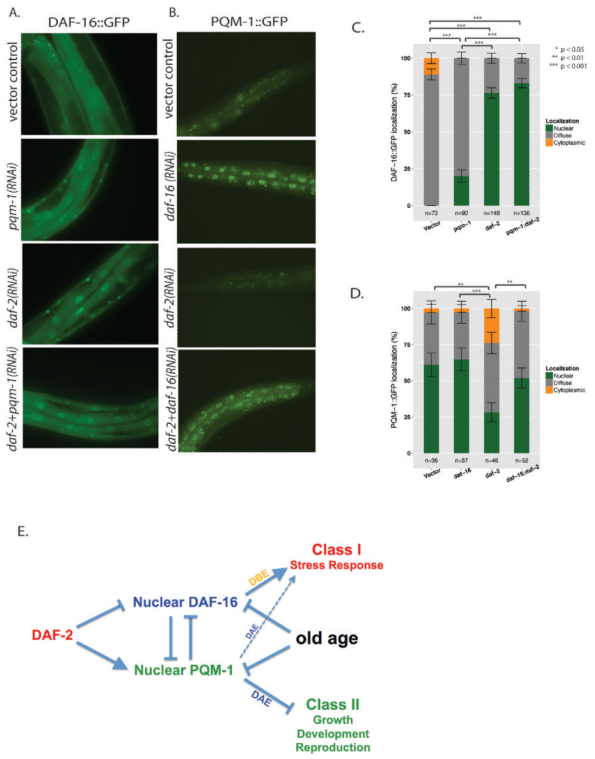

FIGURE 5. PQM-1 and DAF-16 mutually antagonize their nuclear localization

A, C. Loss of *pqm-1* shifts DAF-16 to the nucleus.

B, D. Loss of *daf-16* from a *daf-2* background, in which PQM-1 is more cytoplasmically localized, shifts PQM-1 back to the nucleus.

E. The localization of both DAF-16 and PQM-1 is regulated by insulin signaling, but in opposite directions, and DAF-16 and PQM-1 mutually inhibit each other's nuclear localization.

See also Supplemental Table S3 and S6.

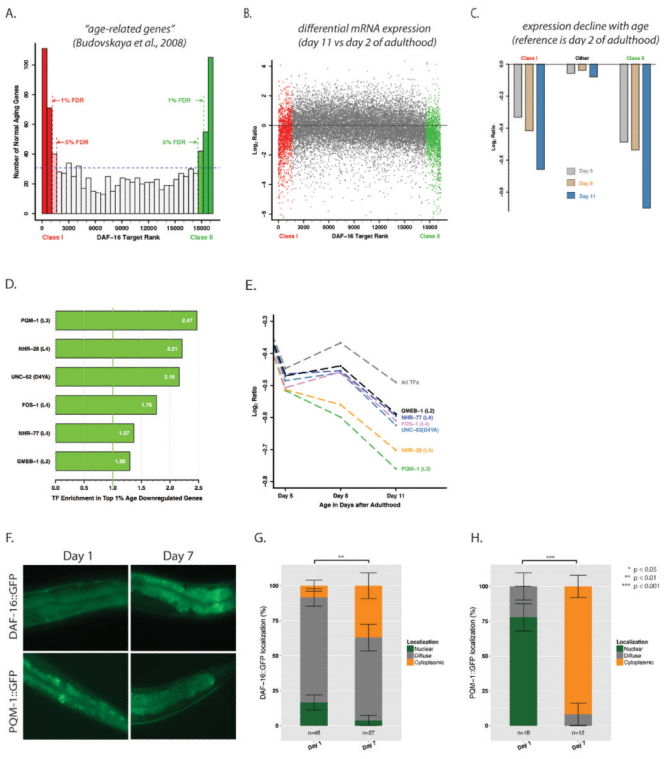

FIGURE 6. PQM-1 is a major regulator of age-related loss of gene expression

A. The distribution of genes classified by Budovskaya et al. (2008) as "age-regulated" versus our ranking shows that our Classes I and II are both strongly affected during normal aging.

B. Differential expression of all genes between day 11 and day 2 of adulthood, shown in the context of our ranking.

C. Expression change (mean log-ratio) for Class I, Class II, and other genes as a function of age, day 2 of adulthood being the reference.

D. Fold-enrichment vs. genome-wide average of ChIP-seq binding sites in the 1% of genes most strongly downregulated with age.

E. Average expression of regulons (sets of targets genes as defined based on ChIP-seq data) for various transcription factors assayed by Niu et al. (2011), shown as a function of advancing age.

F–H. While DAF-16 becomes more cytoplasmic with age, and nuclear localization of PQM-1::GFP decreases significantly with age.

See also Supplemental Table S4

Table 1

Top-50 Class I and Class II DAF-16 responsive genes

	Class I (upregulated)			Class II (downregulated)	
Rank	**Gene**	**Protein Function**	**Rank**	**Gene**	**Protein Function**
1	*mtl-1*	Metallothionein-I	1	*dod-23*	Downstream Of DAF-16
2	F48D6.4a	Unnamed protein	2	*dod-22*	Downstream Of DAF-16; CUB-like domain
3	*hacd-1*	3-hydroxyacyl-CoA dehydrogenase	3	*dod-24*	Downstream Of DAF-16; CUB-like domain
4	*ftn-1*	ferritin heavy chain	4	ZC416.6	leukotriene A4 hydrolase/aminopeptidase
5	*lys-7*	LYSozyme; innate immune reponse	5	F35E12.5	hypothetical protein
6	*dod-6*	Downstream Of DAF-16	6	ZK6.11a	hypothetical protein; DUF274
7	*dod-3*	Downstream Of DAF-16	7	F28H7.3	lipase
8	*btb-16*	BTB (Broad/complex/Tramtrack/Bric a brac)	8	F49F1.1	hypothetical protein
9	M60.4b	hypothetical protein	9	*pept-1*	Oligopeptide transporter (*opt-2*)
10	*gpd-3*	Glyceraldehyde 3-Phosphate Dehydrog'ase	10	*dod-17*	Downstream Of DAF-16
11	E01A2.10	hypothetical protein	11	F19C7.2	lysosomal carboxypeptidase
12	*gpd-2*	Glyceraldehyde 3-Phosphate Dehydrog'ase	12	*dct-18*	DAF-16 controlled, germline tumor affecting
13	T02B5.1	carboxylesterase	13	*clec-209*	C-type LECtin
14	*acs-17*	long-chain-fatty-acid coA ligase (*dod-9*)	14	*ugt-53*	ugt family UDP-GlucuronosylTransferase
15	Y6G8.2	DUF38;F-box domain, cyclin-like	15	F54F11.2a	Zinc-binding metalloprotease
16	*fat-5*	delta-9 fatty acid desaturase, mitochondrial	16	*nuc-1*	DNAse II homolog; apoptotic cell DNA deg.
17	*dao-3*	methylenetetrahydrofolate dehydrogenase	17	*cpr-5*	cysteine thiol protease
18	*cdr-2*	glutathione S-transferase	18	*ncx-6*	Na/Ca,K antiporter
19	*scl-20*	SCP-like extracellular Proteins (*dct-2*)	19	C10C5.4	aminoacylase-1
20	*ugt-41*	ugt family UDP-GlucuronosylTransferase	20	T24B8.5	ShK-like toxin peptide
21	C08E8.4	hypothetical protein	21	C32H11.4	CUB-like domain protein
22	*cyp-35B1*	cytochrome P450 (*dod-13*)	22	cyp-35A3	cytochrome P450
23	F47B8.2	hypothetical protein DUF2700	23	C32H11.9	CUB-like domain protein
24	F09F7.6	hypothetical protein	24	K10D11.5	CUB-like domain protein
25	M01H9.3a	hypothetical protein	25	*nhx-2*	NA(+)/H(+) exchanger
26	*klo-1*	Klotho glycosyl hydrolase	26	*vha-6*	vacuolar ATP synthase
27	F38B6.4	GARS/AIRS/GART	27	*dod-21*	CUB-like domain protein
28	B0286.3	saicar synthetase/air carboxlyase	28	*pho-1*	intestinal acid phosphatase
29	*ttr-26*	Transthyretin-like family	29	T05E12.3	BTB/POZ-like protein domain
30	*nspa-9*	Nematode Specific Peptide family, group A	30	F19C7.4	lysosomal carboxypeptidase
31	ZK355.3	hypothetical protein	31	*oac-6*	O-ACyltransferase homolog
32	E01G4.3a	hypothetical protein	32	*gale-1*	NAD dependent epimerase/dehydratase
33	*spp-12*	SaPosin-like Protein family (*dod-5*)	33	F08G5.6	CUB-like domain protein
34	PDB1.1b	hypothetical cation efflux protein	34	F55G11.8	CUB-like domain protein
35	*pcbd-1*	Pterin CarBinolamine Dehydratase	35	F35E12.9a	CUB-like domain protein
36	*cyp-34A9*	cytochrome P450 (*dod-16*)	36	*oac-20*	O-ACyltransferase homolog
37	*sodh-1*	alcohol dehydrogenase (*dod-11*)	37	F55G11.2	CUB-like domain protein

	Class I (upregulated)			Class II (downregulated)	
Rank	**Gene**	**Protein Function**	**Rank**	**Gene**	**Protein Function**
38	*ttr-44*	Transthyretin-like family	38	*dpyd-1*	human DihydroPYrimidine Dehyd'ase ortholog
39	W01A11.1	epoxide hydrolase	39	F56A4.2	C-type LECtin
40	*sip-1*	Heat shock hsp20 proteins	40	F08A8.2	acyl-coenzyme A oxidase
41	*sod-3*	superoxide dismutase	41	*clec-265*	C-type LECtin
42	F45D11.1	hypothetical protein	42	*pho-8*	histidine acid phosphatase
43	C25E10.8	secreted TIL-domain protease inhibitor	43	T25C12.3	EGF-repeats
44	*icl-1*	isocitrate lyase/malate synthase (*gei-7*)	44	*amt-4*	ammonium transporter
45	*stdh-1*	estradiol 17 beta-dehydrogenase (*dod-8*)	45	C10C5.5	aminoacylase-1
46	C08F11.3	putative O-ACyltransferase homolog	46	*oac-59*	O-ACyltransferase homolog
47	*nspa-3*	Nematode Specific Peptide family, group A	47	*ins-7*	insulin-like peptide; likely DAF-2 agonist
48	*hil-1*	histone H1 like	48	W02B12.1	phospholipase
49	*hen-1*	HEsitatioN LDL receptor motif A secreted prot	49	*nrf-6*	12 TM domains; Nose Resistant to Fluoxetine
50	*ttr-5*	Transthyretin-like family	50	*cyp-13A2*	cytochrome P450

The 50 most significant positive (Class I) and negative (Class II) transcriptional targets of the DAF-16 transcription factor, according to our consensus ranking of all genes in terms of their responsiveness to DAF-16 activity, are shown. See Table S1 for a full ranking of all genes along with DBE and DAE affinity scores.

[a] FDR for all genes $< 10^{-14}$